ACS OMEGA

http://pubs.acs.org/journal/acsodf

Article

Photodynamic Therapy by Glucose Transporter 1-Selective Light Inactivation

Kazuki Miura, Yijin Wen, Michihiko Tsushima, and Hiroyuki Nakamura*

Cite This: *ACS Omega* 2022, 7, 34685−34692

Read Online

ACCESS | Metrics & More | Article Recommendations | Supporting Information

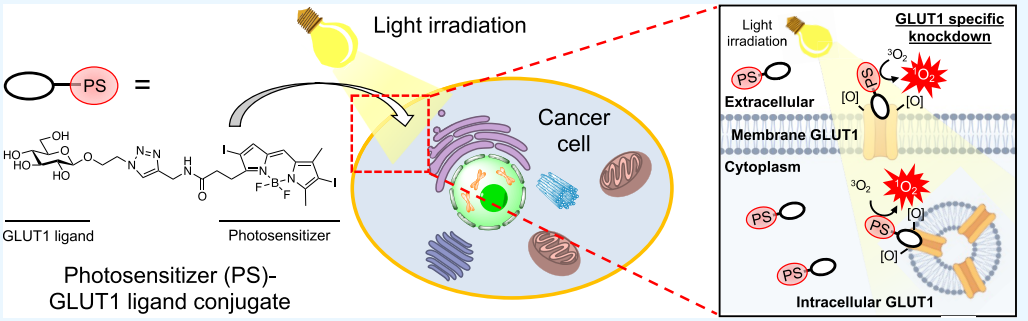

ABSTRACT: Chromophore-assisted light inactivation (CALI) was applied to molecule-targeted photodynamic therapy (PDT). In order to identify organic photosensitizers suitable for CALI, the carbonic anhydrase II (CAII) ligand, 4-sulfamoylbenzoic acid **1**, was conjugated with several photosensitizers to produce compounds **2**−**7**, whose CALI ability was evaluated by measuring their effect on CAII enzymatic activity. Di-iodinated BODIPY (I_2BODIPY) exhibited excellent CAII inactivation ability, similar to that of Ru(bpy)$_3$. The glucose−I_2BODIPY conjugate (**8**) was synthesized as an inactivation of glucose transporter 1 (GLUT1), a protein overexpressed in many cancer cells. Under light irradiation, **8** exhibited concentration-dependent cytotoxicity with half maximal inhibitory concentration (IC_{50}) values of 5.49, 11.14, and 8.73 μM, against human cervical carcinoma (HeLa), human lung carcinoma (A549), and human hepatocellular carcinoma (HepG2) cell lines, respectively. The GLUT1 inhibitor phloretin suppressed the cytotoxicity induced by **8** under light irradiation in a concentration-dependent manner. Western blot analysis indicated that GLUT1 was not detected in cell lines treated with 10 μM **8** under light irradiation. Furthermore, **8** reduced the levels of epidermal growth factor receptor tyrosine kinase (EGFR), phospho-ERK (Y204), and GLUT1 without affecting ERK, α-tubulin, and PCNA protein levels, whereas talaporfin sodium, a clinically approved photosensitizer for PDT, nonspecifically reduced intracellular protein levels in HeLa cells, indicating that **8** has a GLUT1-specific inactivation ability and causes light-induced cytotoxicity by modulating the EGFR/MAPK signaling pathway.

1. INTRODUCTION

Chromophore-assisted light inactivation (CALI) is an innovative approach aimed at specifically inactivating target proteins using photosensitizers that generate reactive oxygen species following irradiation of light.[1] In the CALI approach, small dye-conjugated antibodies and proteins,[2,3] or fluorescent fusion proteins,[4] have been widely employed to achieve the light-triggered oxidative and specific oxidative inactivation of target molecules.[5] Although various dyes have been identified as photosensitizers,[6] tris(bipyridine)ruthenium(II) chloride (Ru(II)(bpy)$_3^{2+}$) has been found to exhibit a high photocatalytic activity for singlet oxygen generation, and the peptoid−ruthenium conjugates have been observed to display significant CALI efficiency in the inactivation of target proteins as a result of visible light irradiation (Figure 1).[7,8] We have also recently reported the ruthenium−photocatalyzed selective CALI of epidermal growth factor receptor tyrosine kinase (EGFR-PTK), which plays an important role in cell growth signaling.[9,10]

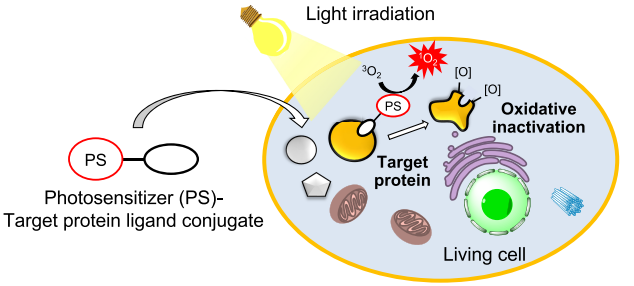

Figure 1. Strategy applied in this study to develop a molecule-targeted photodynamic cancer therapy.

Received: August 7, 2022
Accepted: September 7, 2022
Published: September 16, 2022

ACS Publications

© 2022 The Authors. Published by American Chemical Society

https://doi.org/10.1021/acsomega.2c05042
ACS Omega 2022, 7, 34685−34692

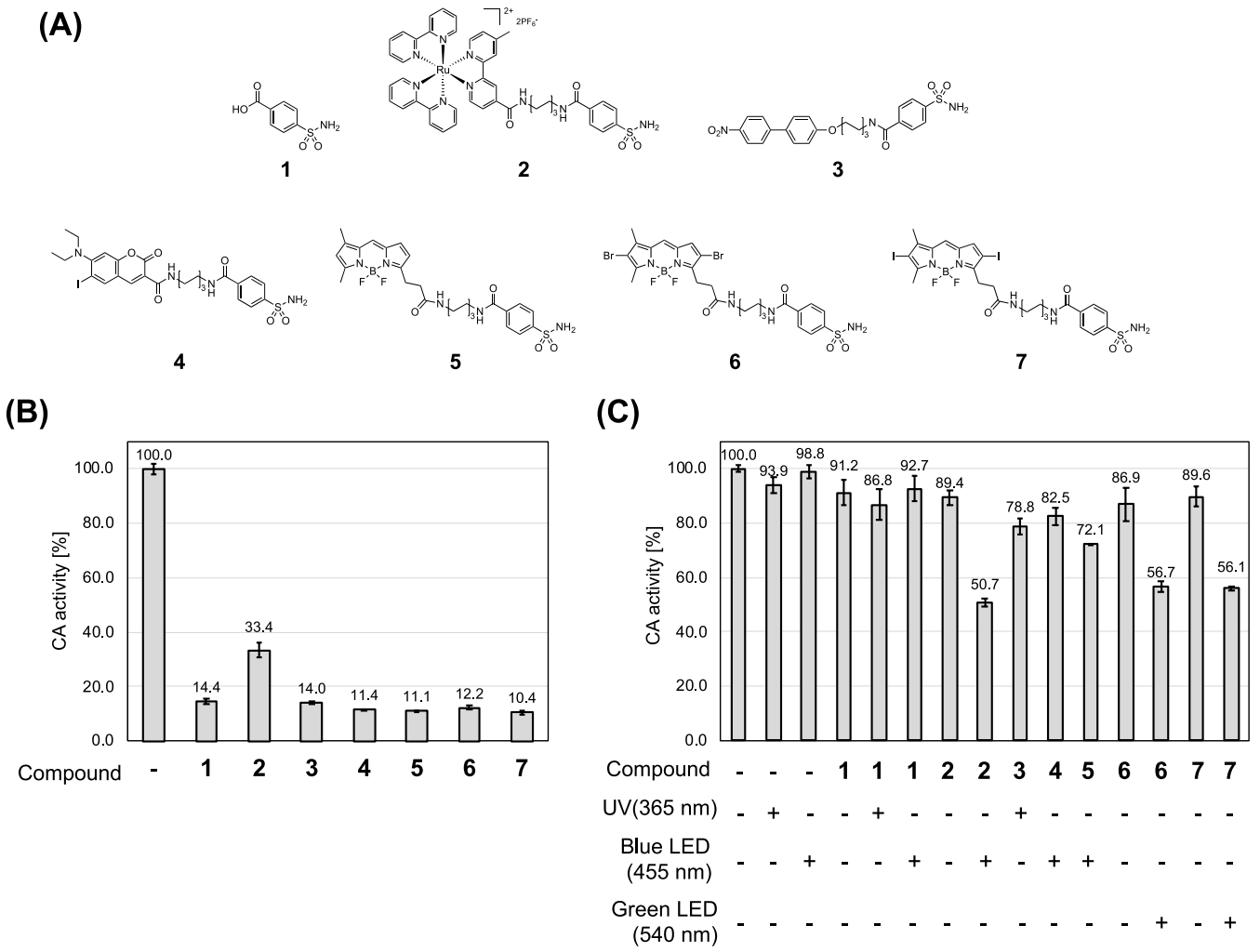

Figure 2. Screening of photosensitizers affording chromophore-assisted light inactivation carried out with the *in vitro* carbonic anhydrase II (CAII) assay system. (A) Structures of the CAII ligand 4-sulfamoylbenzoic acid (**1**) and the **1**-based photosensitizer complexes prepared in this study (**2**−**7**). (B,C) Data reflecting the CAII inhibitory activity of the CAII ligand and of the ligand-derived photosensitizer complexes. The assays were conducted by incubating 1 μM recombinant human CAII in 10 mM MES buffer (pH 7.4) with the solutions of each of the compounds at 4 °C for 1 h; subsequently, (C) the samples were irradiated with light at the indicated wavelengths for 1 h. CAII activity was evaluated by adding 1 mM *p*-nitrophenyl acetate to the reaction mixture and monitoring the obtained solution's absorbance at 340 nm.

Glucose is an important energy source for living cells in the context of ATP production; indeed, glucose is selectively taken up into the cells *via* glucose transporter proteins (GLUTs). Notably, even under aerobic conditions, cancer cells consume large amounts of glucose that is utilized for glycolysis rather than for the oxidative phosphorylation of mitochondria for ATP production, through a phenomenon known as the Warburg effect.[11,12] In fact, various proteins involved in glucose metabolism have been predicted to be attractive molecular targets for cancer therapy, and several inhibitors targeting these proteins are under clinical development as novel cancer therapeutic agents.[13,14] In particular, given that the over-expression of glucose transporter 1 (GLUT1) has been observed in most cancer cells,[15,16] GLUT1 has attracted a great deal of attention as a potential molecular target in cancer therapy.

In this study, we focused on GLUT1 as a target protein for CALI having a goal for the development of photodynamic therapy (PDT), which is a minimally invasive treatment affording the means to damage and destroy localized tumors through the photoactivation of photosensitizers.[17,18] Talaporfin sodium, as a photosensitizer, is widely used in Japan for the clinical treatment of early-stage lung cancers,[19] primary malignant brain tumors,[20] and local residual recurrent esophageal cancers.[21] Recently, cetuximab sarotalocan sodium, an antibody-drug conjugate that combines the anti-epidermal growth factor receptor (EGFR) antibody cetuximab with the photosensitizer IR700, has been approved for the treatment of head and neck cancers.[22−24] Indeed, cetuximab sarotalocan sodium is the first molecule-targeted PDT agent. We speculated that the specific knockdown of GLUT1 might result in cancer cell-specific cytotoxicity. Although several reports have been published on conjugates of glucose and photosensitizers that display tumor-selective accumulation *via* GLUTs,[25,26] the present study represents the first demonstration of PDT based on GLUT1-selective protein knockdown. In detail, we evaluated the protein inactivation ability of several photosensitizers and found di-iodinated boron dipyrromethene (I_2BODIPY) to exhibit excellent protein inactivation activity *in vitro*. Furthermore, glucose-conjugated I_2BODIPY exhibited remarkable antitumor activity *via* specific inactivation of GLUT1 protein in cells, proving the development of the first small molecule-based molecule-targeted PDT agent.

https://doi.org/10.1021/acsomega.2c05042
ACS Omega 2022, 7, 34685−34692

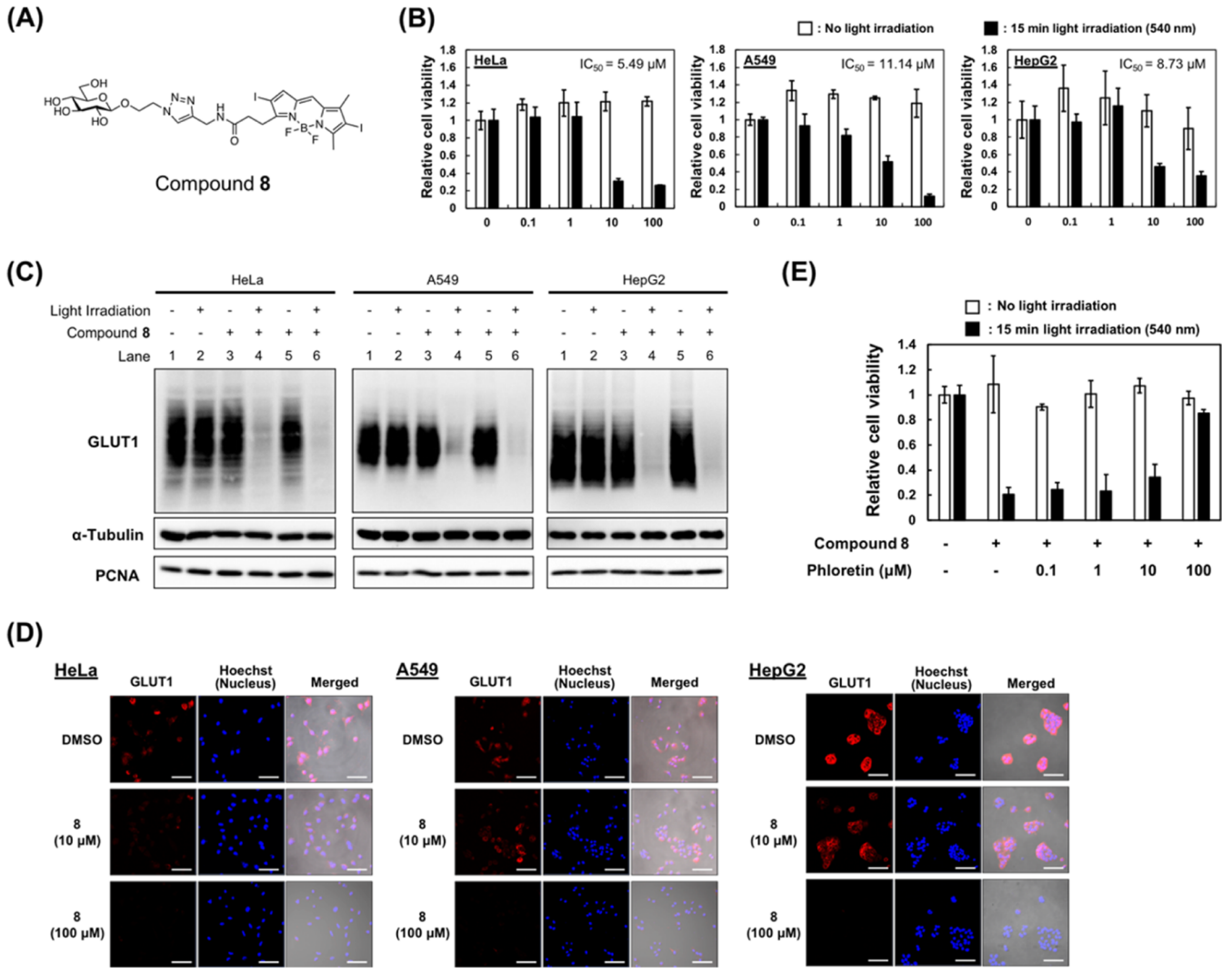

Figure 3. Evaluation of the bioactivity of compound **8** for chromophore-assisted light inactivation targeting glucose transporter 1 (GLUT1) in cancer cells. (A) Structure of compound **8**. (B) Data reflecting the antitumor activity of compound **8**. Cells (HeLa, A549, and HepG2) were cultured in a 96-well plate and treated with compound **8** at the indicated concentrations for 1 h. The cells were then washed with phosphate-buffered saline (PBS) and irradiated with light at 540 nm wavelength. After 72 h of culture in Dulbecco's modified Eagle's medium (DMEM), thiazolyl blue tetrazolium bromide (MTT) to a final concentration of 0.5 mg/mL was added to the cell cultures, which were then incubated for 4 h at 37 °C. The medium was removed, and the MTT formazan product was dissolved in dimethyl sulfoxide (DMSO). The amount of this product was determined by measuring the absorbance at 570 nm using a microplate reader. IC_{50}: half maximal inhibitory concentration. (C) Results of the western blot analyses conducted to evaluate the light irradiation-dependent protein knockdown ability of compound **8**. Cells were treated with 10 μM compound **8** or a blank solution for 1 h and then washed with PBS; they were then irradiated with light at 540 nm wavelength for 15 min (lanes 2 and 4) or 30 min (lane 6). The cells were subsequently lysed at 4 °C by sonication, and the resulting samples were electrophoresed on sodium dodecyl sulfate (SDS)−polyacrylamide gel and transferred to polyvinylidene difluoride membranes. The samples thus obtained were immunoblotted with anti-GLUT1, anti-α-tubulin, and anti-PCNA antibodies. (D) Results of the evaluation of the ability of compound **8** to effect the light irradiation-dependent knockdown of GLUT1 by immunofluorescence analysis. Cells were treated with 10 μM compound **8** or a blank solution for 1 h and then washed with PBS; they were irradiated with light at 540 nm wavelength for 15 min. The cells were fixed, and then, the samples were immunoblotted with anti-GLUT1 antibody. Scale bars: 100 μm. (E) Results of GLUT1 inhibitor phloretin competition assays conducted on compound **8**. Cells were cultured in a 96-well plate and treated with 10 μM compound **8** and phloretin at the indicated concentrations for 10 min. The cells were washed with PBS and irradiated with light at 540 nm wavelength for 15 min. After 72 h culture in DMEM, MTT was added to a final concentration of 0.5 mg/mL, and the resulting cell culture was incubated for 4 h at 37 °C. The medium was removed, and the MTT formazan product was dissolved in DMSO. The amount of MTT formazan was determined by measuring the absorbance at 570 nm using a microplate reader.

2. RESULTS AND DISCUSSION

2.1. Screening of Photosensitizers for CALI. In a previous published study, we determined that several organic photocatalysts generate radical species by singlet electron transfer with excellent cell permeability in intracellular photocatalytic-proximity labeling (iPPL).[27] However, whether or not these photocatalysts are effective for CALI remains unclear. Therefore, in order to investigate this issue, herein, carbonic anhydrase II (CAII) was selected as a target protein model and 4-sulfamoylbenzoic acid (**1**) as its ligand; indeed, the protein inactivation ability of **1** implemented the *in vitro* CAII enzymatic assay. Because CAII exhibits esterase activity, its enzymatic activity was measured by detecting its ability to hydrolyze *p*-nitrophenyl acetate.[28] First, we designed and synthesized the CAII ligand-conjugated photosensitizers **2**−**7** (Figure 2A).

https://doi.org/10.1021/acsomega.2c05042
ACS Omega 2022, 7, 34685−34692

$Ru(bpy)_3$ is a well-known photosensitizer used for CALI that causes oxidative damage against biomolecules *via* singlet oxygen production and photo-induced electron transfer by light irradiation, and its CAII ligand-conjugate **2** was used as a positive control in the CAII inactivation investigation.[7−10] The 4-nitrobiphenyl moiety of compound **3** was found by Yuasa and co-workers as a low molecular weight photosensitizer to be characterized by a significant photosensitizing ability resulting from the intersystem crossing of a twist-assisted spin−orbit charge transfer.[29] Coumarin, which is present as a moiety in compound **4**, and/or BODIPY, which is present in compounds **5**−**7**, has been observed to be highly cell permeable and to produce high levels of singlet oxygen.[27] In particular, the di-brominated and di-iodinated BODIPY derivatives **6** and **7**, respectively, were expected to accommodate higher excitation wavelengths.[30] Details of the synthesis of these compounds are described in the Materials and Methods and Supporting Information.

Next, we evaluated the inhibitory effect of CAII ligand-conjugated photosensitizers **2**−**7** on the enzymatic activity of CAII. In detail, CAII was incubated in the presence of each of the photosensitizers, in the same equivalent molar ratio, for 1 h at 4 °C, and then the CAII activity was measured based on the absorbance of *p*-nitrophenyl acetate at 340 nm. As shown in Figure 2B, all compounds except **2** exhibited a level of CAII inhibitory activity with similar levels to that of ligand **1** (*ca.* 90% inhibition). On the other hand, compound **2** exhibited lower inhibitory activity (*ca.* 70% inhibition). These results indicate that the synthesized compounds **3**−**7** bind to CAII and inhibit its enzymatic activity to a similar level as **1**. Notably, the fact that compound **2** displayed a lower CAII inhibitory activity than the other compounds may be due to the molecular size of the $Ru(bpy)_3$ complex. In fact, the relatively large molecular size of this complex may suppress its binding to the CAII enzymatic pocket, resulting in a reduction of the CAII inhibitory activity of compound **2** with respect to those of compounds **3**−**7**.

We subsequently evaluated the protein-inactivating activity of the synthesized compounds **2**−**7** as photosensitizers. CAII was incubated with 10 equivalents of the various compounds, and the reaction mixtures were irradiated with light of the appropriate wavelength for each photosensitizer; specifically, the excitation wavelength of compounds **1** and **3** was at 365 nm; that of compounds **2**, **4**, and **5** was at 455 nm; and that of compounds **6** and 7 was at 540 nm (see Table S1, Figures S1 and S2). Afterward, the enzymatic activity of CAII was measured by spectrophotometrically monitoring the concentration of *p*-nitrophenyl acetate. The results are summarized in Figure 2C. Among the compounds synthesized, **2**, **6**, and **7** exhibited significant inhibition of CAII enzymatic activity, with the original activity dropping to 50.7, 56.7, and 56.1%, respectively, under light irradiation; by contrast, compounds **3**−**5** afforded a lower level of CAII inactivation than compounds **2**, **6**, and **7**. These results indicate that the compounds comprising the dibrominated and di-iodinated BODIPY moieties (compounds **6** and **7**, respectively) are characterized by excellent protein inactivation abilities, which are similar in magnitude to that of the compound comprising the $Ru(bpy)_3$ moiety (compound **2**). In addition, these BODIPY derivatives achieved CAII inactivation by being subjected to irradiation with light at 540 nm wavelength, which is longer than the wavelength utilized in the case of the $Ru(bpy)_3$ complex.

2.2. CALI Targeting GLUT1. Because di-iodinated BODIPY (I_2BODIPY) was found to possess an excellent protein inactivation ability in the screening of photosensitizers for CALI, we went on to investigate protein inactivation targeting GLUT1, a glucose transporter known to be overexpressed in many cancer cells. We designed compound **8** as a photosensitizer targeting GLUT1, and we synthesized it from glucose azide and alkynyl I_2BODIPY implementing a Cu-catalyzed click reaction (Figure 3A). Notably, the attachment of glucose to I_2BODIPY was found to have no effect on singlet oxygen production ability of I_2BODIPY; in fact, compound **8** exhibited excellent singlet oxygen production ability (Figure S3). Compound **8** was then utilized in cell viability experiments conducted using three human cancer cell lines known to overexpress GLUT1: HeLa (human cervical carcinoma), A549 (human lung carcinoma), and HepG2 (human hepatocellular carcinoma) cells. Cell viability was measured by implementing the 3-(4,5-dimethylthiazol-2-yl)-2,5-diphenyltetrazolium bromide (MTT) assay. As shown in Figure 3B, under light irradiation, compound **8** exhibited a concentration-dependent cytotoxicity against these cancer cell lines; however, such cytotoxicity was not observed in the absence of light irradiation. Interestingly, I_2BODIPY itself exhibited strong cytotoxicity against these human cancer cell lines even in the absence of light irradiation (Figure S4). These results indicate that compound **8** possesses sufficient photosensitizing ability to exhibit significant cytotoxicity and that the glucose conjugation contributes to the suppression of the cytotoxicity of I_2BODIPY.

In order to determine whether the light-induced cytotoxicity of compound **8** was caused by the inactivation of GLUT1, we performed western blot analysis of GLUT1 expression in cells incubated in the presence of compound **8**, with and without light irradiation. As shown in Figure 3C, GLUT1 was not detected in the cell lines treated with compound **8** under light irradiation (lanes 4 and 6), whereas GLUT1 was detected in cells treated with compound **8** at 10 μM concentration, under no light irradiation (lanes 3 and 5), in cells subjected to light irradiation in the absence of compound **8** (lane 2), and in cells in the negative control (lane 1). We also measured the GLUT1 protein expression in each cell line by immunostaining using an anti-GLUT1 antibody. As shown in Figure 3D, a reduction in the intensity of the fluorescent signals due to GLUT1 was observed in the cells treated with compound **8**. These results demonstrate that compound **8** selectively interacts with GLUT1 and oxidizes it under light irradiation, resulting in the conversion of GLUT1 into a derivative that is undetectable by immunoblotting analysis. Although GLUT1 is a membrane protein, it has been reported that its subcellular localization switches to the endosomes in response to intracellular glucose concentration.[31] In fact, fluorescence signals due to GLUT1 were also observed intracellularly (Figure 3D; DMSO control), and the accumulation of compound **8** was observed inside the cells (Figure S5). Hence, both membrane-localized and intracellular GLUT1 proteins were oxidatively inactivated. Finally, we determined whether the light-induced cytotoxicity of compound **8** was suppressed by the addition of a GLUT1 inhibitor. Phloretin is a well-known GLUT1 inhibitor that suppresses glucose transport into the cells.[32,33] Thus, phloretin was expected to reduce the light-induced cytotoxicity of compound **8** by inhibiting the binding of this compound to GLUT1. As expected, phloretin suppressed the cytotoxicity induced by compound **8** under light irradiation in a concentration-dependent manner (Figure 3E). These results provide evidence that the cytotoxicity caused by compound **8** is due to the light-induced inactivation of GLUT1.

https://doi.org/10.1021/acsomega.2c05042
ACS Omega 2022, 7, 34685−34692

2.3. Investigating whether Compound 8 Antitumor Activity Is Mediated by the EGFR/MAPK Signaling Pathway. GLUT1 promotes cell proliferation, migration, and invasion *via* regulation of the EGFR/MAPK and integrin β1/Src/FAK signaling pathways in cancer cells.[34] To determine whether the light-induced cytotoxicity of compound **8** is mediated by a GLUT1-related signal pathway, we evaluated the effect of the CALI of GLUT1 on the EGFR/MAPK signal pathway. Talaporfin sodium, a photosensitizer approved as a PDT drug, exhibited antitumor activity by oxidizing various molecules in cells, so it was herein used as a control (Figure S6).[35,36] HeLa cells were incubated with compound **8** or talaporfin sodium under light irradiation at the appropriate wavelength for either compound as described above, and the protein levels were measured by performing western blot analysis. As shown in Figure 4, compound **8** reduced the levels of EGFR, phospho-ERK (Y204), and GLUT1 in the cells, whereas the levels of ERK, α-tubulin, and PCNA were not affected by compound **8**. On the other hand, talaporfin sodium resulted in the nonspecific reduction of intracellular protein levels. These results suggest that the PDT mechanisms of compound **8** and sodium talaporfin are different, with compound **8** suppressing cancer cell proliferation by selective oxidative inactivation of GLUT1 and inhibition of its downstream EGFR/MAPK signaling pathway, whereas talaporfin sodium suppresses cancer cell proliferation by oxidative inactivation of various intracellular proteins, indicating that compound **8** exhibits an ability to specifically inactivate GLUT1 and causes light-induced cytotoxicity by modulating the EGFR/MAPK signaling pathway.

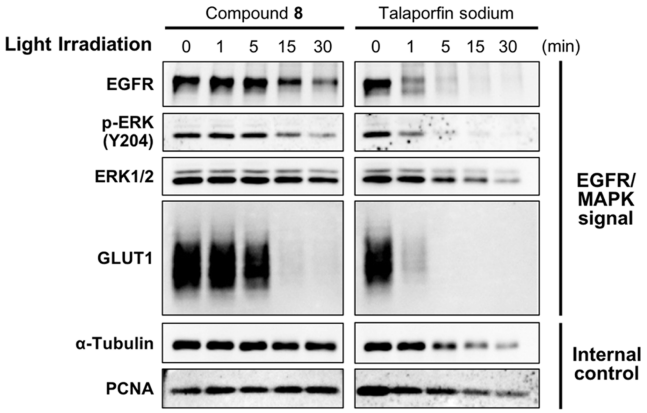

Figure 4. Results of the investigation aimed at identifying the intracellular signaling pathway involved in the knockdown of glucose transporter 1 (GLUT1) by compound **8**. Cells were treated with compound **8** or talaporfin sodium for 1 h and then washed with phosphate-buffered saline; they were then irradiated with light at the indicated wavelengths. The cells were lysed at 4 °C by sonication; the sample was then electrophoresed on sodium dodecyl sulfate-polyacrylamide gel and transferred to polyvinylidene difluoride membranes. The samples thus obtained were immunoblotted with anti-EGFR, anti-ERK1/2, anti-phospho-ERK (Tyr204), anti-GLUT1, anti-α-tubulin, and anti-PCNA antibodies.

3. CONCLUSIONS

We hereby demonstrated intracellular CALI for molecule-targeted PDT. A photosensitizer characterized by high singlet oxygen production and cell membrane permeability is essential for the molecule-targeted PDT. We synthesized several CAII ligand-conjugated photosensitizers and evaluated their protein inactivation ability using CAII as a protein inactivation model *in vitro*. I_2BODIPY was found to exhibit excellent protein inactivation ability under the irradiation of light at 540 nm wavelength. Moreover, we synthesized a glucose-conjugated I_2BODIPY, compound **8**, which was observed to target GLUT1 for cancer cell-specific molecule-targeted PDT. We found compound **8** to afford excellent GLUT1-specific protein inactivation, without affecting other housekeeping proteins, such as α-tubulin and PCNA; indeed, treatment with compound **8** resulted in significant light-induced cytotoxicity mediated by modulation of the EGFR/MAPK signaling pathway. These results demonstrate the potential of a novel molecule-targeted PDT and postulate spatiotemporally controllable drug discovery through the light-induced selective inactivation of tumor-specific proteins.

4. MATERIALS AND METHODS

4.1. Synthesis of CAII Ligand-Conjugated Ru(bpy)$_3$ Complex (2). Compound **2** was synthesized according to the previously reported procedure.[37]

4.2. Synthesis of CAII Ligand-Conjugated 4-Nitrobiphenyl Complex (3). Compound **15** (36.2 mg, 0.18 mmol) was dissolved in 2 mL of dimethylformamide (DMF), and to the obtained solution were added 4-sulfomoylbenzoic acid (21 mg, 0.10 mmol), EDCI·HCl (21.4 mg, 0.14 mmol), HOBT·H_2O (23.3 mg, 0.17 mmol), and DIEA (29.8 mg, 0.23 mmol). After stirring the obtained mixture at room temperature overnight, it was poured into ethyl acetate (EtOAc). The organic layer was washed with saturated $NaHCO_3$ (aq) and dried over Na_2SO_4. The crude product was purified by column chromatography on silica gel (eluent, hexane/EtOAc = 1:3) to obtain compound **3** as a pale yellow solid (33.4 mg, 0.07 mmol; yield, 58%). ^{1}H NMR (400 MHz, DMSO-d_6): δ 8.64 (1H, t, J = 5.2 Hz), 8.27 (2H, d, J = 8.8 Hz), 7.99 (2H, d, J = 8.2 Hz), 7.90 (4H, t, J = 8.3 Hz), 7.74 (2H, d, J = 9.0 Hz), 7.47 (2H, s), 7.08 (2H, d, J = 8.2 Hz), 4.04 (2H, t, J = 6.5 Hz), 3.29 (2H, t, J = 6.3 Hz), 1.80−1.71 (2H, m), 1.61−1.53 (2H, m), 1.52−1.35 (4H, m); ^{13}C NMR (125 MHz, DMSO-d_6): δ 165.55, 160.12, 146.79, 146.59, 146.49, 138.10, 131.89, 130.28, 129.02 (x2), 128.24 (x2), 127.43 (x2), 126.04 (x2), 124.54 (x2), 115.66 (x2), 68.14, 29.39, 29.02, 26.68, 25.73; HRMS (ESI, Positive): m/z calcd. for $C_{25}H_{27}N_3O_6S$, $[M + Na]^+$: 520.1513; found, 520.1523. Purity: 99.7% [Reverse-phase HPLC (C18 column), retention time = 18.40 min, 20−50% MeCN/H_2O containing 0.1% formic acid].

4.3. Synthesis of CAII Ligand-Conjugated Coumarin Complex (4). Compound **18** (19.4 mg, 0.05 mmol) was dissolved in 2 mL of DMF, and to the obtained solution were added *N*-(6-aminohexyl)-4-sulfamoylbenzamide (**11**; 15 mg, 0.05 mmol), EDCI·HCl (11.5 mg, 0.06 mmol), and HOBT·H_2O (11.5 mg, 0.08 mmol). After stirring the obtained mixture at room temperature overnight, it was poured into EtOAc. The organic layer was washed with ice water, 1 M HCl (aq), and saturated $NaHCO_3$ (aq); it was then dried over Na_2SO_4. The crude product was purified by GPC (eluent, dichloromethane/methanol = 10:1) to obtain compound **4** as a yellow solid (19.6 mg, 0.03 mmol; yield, 59%). ^{1}H NMR ($CDCl_3$, 500 MHz): δ 8.79 (1H, t, J = 5.7 Hz), 8.67 (2H, s), 8.09 (2H, s), 7.76 (2H, s), 6.91 (2H, s), 6.04 (1H, s), 3.41 (4H, s), 3.22 (4H, q, J = 7.0 Hz), 1.63−1.54 (5H, m), 1.40 (5H, d, J = 0.7 Hz), 1.25 (3H, s), 1.10 (1H, t, J = 7.1 Hz); ^{13}C NMR (125 MHz, $CDCl_3$): δ 166.6, 162.1, 161.7, 158.2, 155.5, 147.1, 144.8, 141.2, 138.4, 127.9, 126.4, 115.7, 115.4, 109.7, 91.4, 46.8 (x2), 40.2, 39.7, 29.8, 29.3,

https://doi.org/10.1021/acsomega.2c05042
ACS Omega 2022, 7, 34685−34692

29.2, 26.4, 26,3, 12.3 (x3). HRMS (ESI, Positive): m/z calcd. for $C_{27}H_{33}IN_4O_6S$, $[M + Na]^+$: 691.1058; found, 691.1059. Purity: 99.5% [Reverse-phase HPLC (C18 column), retention time = 18.03 min, 20−50% MeCN/H_2O containing 0.1% formic acid].

4.4. Synthesis of CAII Ligand-Conjugated BODIPY Complex (5). Compound **23** (38 mg, 0.12 mmol) was dissolved in 5 mL of DMF, and to the obtained solution were added EDCI·HCl (30 mg, 0.15 mmol) and HOBT·H_2O (30 mg, 0.19 mmol). After stirring the obtained mixture at room temperature for 10 min, **11** (43 mg, 0.14 mmol) was added to it. The mixture was then further stirred overnight at room temperature and poured into EtOAc. The organic layer was washed with ice water, saturated NH_4Cl (aq), saturated $NaHCO_3$ (aq), and brine; it was then dried over Na_2SO_4. The crude product was purified by column chromatography on silica gel (eluent, dichloromethane/methanol = 15:1) to obtain compound **5** as a red solid (47.8 mg, 0.08 mmol; yield, 65%). ^{1}H NMR (400 MHz, $CDCl_3$): δ 8.62 (1H, t, J = 5.2 Hz), 7.98 (2H, d, J = 8.6 Hz), 7.89 (3H, d, J = 8.4 Hz), 7.68 (1H, s), 7.47 (2H, s), 7.09 (1H, d, J = 3.9 Hz), 6.35 (1H, d, J = 4.2 Hz), 6.30 (1H, s), 3.26 (2H, q, J = 6.4 Hz), 3.11−3.03 (4H, m), 2.48 (3H, s), 2.26 (3H, s), 1.58−1.48 (3H, m), 1.45−1.37 (2H, m), 1.36−1.21 (5H, m); ^{13}C NMR (125 MHz, DMSO-d_6): δ 171.06, 165.54, 159.56, 158.41, 146.56, 144.51, 138.09, 134.89, 133.45, 129.36, 128.24 (x2), 126.04 (x2), 125.76, 120.71, 117.06, 38.94, 34.26, 29.54, 29.44 (x2), 26.66, 26.60, 24.52, 14.95, 11.44; HRMS (ESI, Positive): m/z calcd. for $C_{27}H_{34}BF_2N_5O_4S$, $[M + Na]^+$: 596.2290; found, 596.2281. Purity: 97.4% [Reverse-phase HPLC (C18 column), retention time = 2.75 min, 50% MeCN/H_2O containing 0.1% formic acid].

4.5. Synthesis of CAII Ligand-Conjugated di-bromination BODIPY Complex (6). Compound **25** (29 mg, 0.07 mmol) was dissolved in 3 mL of DMF, and to the obtained solution were added EDCI·HCl (15 mg, 0.08 mmol) and HOBT·H_2O (15 mg, 0.09 mmol). After stirring the mixture thus obtained at room temperature for 10 min, **11** (21.4 mg, 0.07 mmol) was added to it. The mixture was further stirred overnight at room temperature and poured into EtOAc. The organic layer was washed with ice water, saturated NH_4Cl (aq), saturated $NaHCO_3$ (aq), and brine; it was then dried over Na_2SO_4. The crude product was purified by column chromatography on silica gel (eluent, dichloromethane/methanol = 15:1) to obtain compound **6** as a red solid (31.2 mg, 0.04 mmol; yield, 66%). ^{1}H NMR (DMSO-d_6, 500 MHz): δ 8.63 (1H, t, J = 5.6 Hz), 8.32 (0H, s), 7.99 (1H, d, J = 7.9 Hz), 7.90 (3H, d, J = 7.9 Hz), 7.69 (1H, s), 7.48 (2H, s), 7.09 (1H, d, J = 3.9 Hz), 6.35 (1H, d, J = 3.7 Hz), 6.30 (1H, s), 3.27 (4H, q, J = 6.7 Hz), 3.08 (2H, q, J = 6.3 Hz), 2.26 (2H, s), 1.53 (2H, t, J = 7.2 Hz), 1.41 (2H, t, J = 6.8 Hz), 1.31 (5H, s). ^{13}C NMR (125 MHz, DMSO): δ 171.07, 165.54, 146.55. 138.06, 134.89, 133.43, 129.38, 128.26 (x2), 126.05 (x3), 125.79, 120.73, 117.07, 79.63, 38.93, 34.23, 29.55 (x2), 29.43, 26.66 (x2), 26.60, 24.50, 14.97, 11.45. HRMS (ESI, Positive): m/z calcd. for $C_{27}H_{32}BF_2I_2N_5O_4S$, $[M + Na]^{+:}$ 754.0481; found, 754.0482. Purity: 94.3% [Reverse-phase HPLC (C18 column), retention time = 1.33 min, 50% MeCN/H_2O containing 0.1% formic acid].

4.6. Synthesis of CAII Ligand-Conjugated Di-iodination BODIPY Complex (7). Compound **27** (29 mg, 0.05 mmol) was dissolved in 5 mL of DMF, and to the obtained solution were added EDCI·HCl (13 mg, 0.07 mmol) and HOBT·H_2O (13 mg, 0.08 mmol). After stirring the thus obtained mixture at room temperature for 10 min, **11** (18 mg, 0.06 mmol) was added to it. The mixture was then further stirred overnight at room temperature and poured into EtOAc. The organic layer was washed with ice water, saturated NH_4Cl (aq), saturated $NaHCO_3$ (aq), and brine; it was then dried over Na_2SO_4. The crude product was purified by column chromatography on silica gel (eluent, dichloromethane/methanol = 15:1) to obtain compound **7** as a red solid (21 mg, 0.03 mmol; yield, 63%). ^{1}H NMR (DMSO-d_6, 500 MHz): δ 8.63 (1H, t, J = 5.6 Hz), 7.99 (1H, d, J = 8.6 Hz), 7.99 (1H, d, J = 8.6 Hz), 7.90 (2H, d, J = 8.0 Hz), 7.89 (2H, d, J = 8.6 Hz), 7.83 (1H, s), 7.82 (1H, s), 7.48 (2H, s), 7.40 (1H, s), 3.27 (2H, q, J = 6.7 Hz), 3.07 (2H, q, J = 6.2 Hz), 2.53 (3H, s), 2.37 (2H, t, J = 8.6 Hz), 2.22 (2H, s), 1.54 (2H, t, J = 6.9 Hz), 1.43 (2H, t, J = 6.9 Hz), 1.28 (5H, t, J = 23.5 Hz); ^{13}C NMR (125 MHz, DMSO-d_6): δ 170.27, 165.55, 160.54, 158.17, 147.89, 146.82, 146.47, 138.07, 135.94, 134.64, 128.24 (x2), 126.04 (x2), 86.01, 79.53, 76.10, 39.03, 34.23, 29.54 (x2), 29.40, 26.65 (x2), 24.91, 16.17, 13.99. HRMS (ESI, Positive): m/z calcd. for $C_{27}H_{32}BF_2I_2N_5O_4S$, $[M + Na]^+$: 848.0223; found, 848.0225. Purity: 98.7% [Reverse-phase HPLC (C18 column), retention time = 1.48 min, 70% MeCN/H_2O containing 0.1% formic acid].

4.7. Synthesis of GLUT1 Ligand Glucose-Conjugated Di-iodination BODIPY Complex (8). 2-Azidoethyl β-D-glucopyranoside (20 mg, 0.08 mmol), $CuSO_4·5H_2O$ (17 mg, 0.07 mmol), and L-ascorbic acid sodium salt (14 mg, 0.07 mmol) were dissolved in 5 mL of H_2O, and to the obtained solution was added a solution of compound **28** (40 mg, 0.07 mmol) in 7 mL of tetrahydrofuran (THF). After stirring the obtained mixture at room temperature for 45 min, it was poured into EtOAc. The biphasic mixture thus obtained was extracted using a separatory funnel, and the organic layer was separated; the said layer was then washed with brine and subsequently dried over brine and Na_2SO_4. The crude product was purified by column chromatography on silica gel (eluent, dichloromethane/methanol = 10:1) to obtain compound **8** as a dark red amorphous solid. (8.7 mg, 0.01 mmol, 14%). ^{1}H NMR (CH_3OD, 400 MHz): δ 8.44 (1H, s), 8.03 (1H, s), 7.58 (1H, s), 7.30 (1H, s), 4.65 (1H, t, J = 4.9 Hz), 4.48 (1H, s), 4.33 (2H, s), 4.29−4.23 (2H, m), 4.06−3.97 (1H, m), 3.88 (1H, d, J = 10.4 Hz), 3.76−3.50 (3H, m), 3.30 (2H, s), 3.22 (3H, dd, J = 9.3, 17.5 Hz), 2.61 (2H, s), 2.28 (2H, s), 1.32 (6H, s); ^{13}C NMR (125 MHz, DMSO): δ 170.86, 160.80, 157.62, 148.12, 136.00, 134.54, 125.44, 124.33, 103.29, 85.13, 81.50, 77.17, 76.88, 76.24, 73.68 (x2), 70.44, 67.84, 61.50, 50.17, 34.68, 34.00, 24.76, 16.12, 13.93. HRMS (ESI, Positive): m/z calcd. for $C_{25}H_{31}BF_2I_2N_6O_7$, $[M + Na]^+$: 853.0301; found, 853.0322. Purity: 98.0% [Reverse-phase HPLC (C18 column), retention time = 6.41 min, 50% MeCN/H_2O containing 0.1% formic acid].

4.8. *In Vitro* Assay. All compounds were prepared as 10 mM DMSO solutions, which were subsequently diluted to the indicated concentrations using 10 mM MES buffer (pH 7.4). The assays were conducted by incubating a 1 μM recombinant human CAII solution and each compound solution at 4 °C for 1 h; afterward, the mentioned solutions were irradiated with light at the appropriate wavelength. Subsequently, CAII activity was evaluated by adding 1 mM p-nitrophenyl acetate to the reaction mixture and monitoring the solution's absorbance at 340 nm. In order to prepare the blank, the p-nitrophenyl acetate solution was replaced by the pure 10 mM MES buffer. The CAII activity was defined as follows: absorbance = absorbance of compounds treatment − absorbance of blank. The relative rate of CAII

https://doi.org/10.1021/acsomega.2c05042
ACS Omega 2022, 7, 34685−34692

activity was expressed by comparison with the absorbance that was obtained from compound non-treatment at 20 min, which was taken as 100%.

4.9. Cell Cultures. Human cervical carcinoma HeLa cells, human lung carcinoma A549 cells, and human hepatocellular carcinoma HepG2 cells were cultured in Dulbecco's modified Eagle's medium (DMEM; FUJIFILM Wako Pure Chemical Corporation, Japan) that was supplemented with 10% (v/v) fetal bovine serum and 1% penicillin/streptomycin solution (Thermo Fisher Scientific, Inc., USA) at 37 °C in 5% CO_2.

4.10. MTT Assay. Cells were cultured in a 96-well plate and treated with the various compounds for 1 h. They were then washed with phosphate-buffered saline (PBS) and irradiated with light at the indicated wavelength. After 72 h of culture in DMEM, 0.5 mg/mL MTT (Merck KGaA) was added to the DMEM culture, which was then incubated for 4 h at 37 °C. The medium was then removed, and the MTT formazan product was dissolved in DMSO. The amount of MTT formazan product was determined by measuring the absorbance of the DMSO solution at 570 nm using a microplate reader (Infinite F200, Tecan Japan Co., Ltd., Japan).

4.11. Western Blot. Cells were treated with the various compounds for 1 h and then washed with PBS; subsequently, they were irradiated with light at the indicated wavelength. Afterward, the cells were lysed using the RIPA buffer, which consisted of 50 mM Tris−HCl (pH 8.0), 150 mM sodium chloride, 0.5% (w/v) sodium deoxycholate, 0.1% (w/v) sodium dodecyl sulfate (SDS), 1.0% (w/v) NP-40 substitute, and protease inhibitor cocktail (Sigma-Aldrich, USA), at 4 °C under sonication. The amounts of proteins present in each lysate were measured utilizing the BCA protein assay reagent (Thermo Fisher Scientific, Inc., USA). A 5× sample buffer consisting of 250 mM Tris−HCl (pH 6.8), 625 mM 2-mercaptoethanol, 10% (w/v) SDS, 0.125% (w/v) bromophenol blue (BPB), and 10% (w/v) glycerol was added to each cell lysate. The mixtures thus obtained were boiled at 98 °C for 5 min, electrophoresed on SDS-polyacrylamide gel, and transferred to polyvinylidene difluoride membranes. These obtained samples were immunoblotted with anti-EGFR (#sc-03, Santa Cruz Biotechnology, Inc., USA), anti-ERK1/2 (#ADI-KAP-MA001, Enzo Life Sciences, Inc., USA), anti-phospho-ERK (Tyr204) (#sc-7976, Santa Cruz Biotechnology, Inc., USA), anti-GLUT1 (#ab115730, abcam, UK), anti-α-tubulin (#013-25033, FUJIFILM Wako Pure Chemical Corporation, Japan), and anti-PCNA (#60097-1-Ig, Proteintech, USA) antibodies. Signals were detected with ECL using ImmunoStar LD (FUJIFILM Wako Pure Chemical Corporation, Japan) or Immobilon Forte Western HRP substrates (Merck KGaA, USA).

4.12. Immunofluorescence. Cells were treated with the various compounds for 1 h and washed with PBS; subsequently, they were irradiated with light at the indicated wavelength. Next, the cells were fixed by treating them with PBS containing 4% paraformaldehyde for 20 min and permeabilized by treating them with 0.1% (v/v) Triton X-100 for 10 min. After blocking with 2% bovine serum albumin for 30 min, the fixed cells were incubated with mouse anti-GLUT1 antibody and Alexa Fluor 647-conjugated goat anti-mouse IgG (#ab150115, abcam, UK) for 1 h. The fluorescence signals were recorded using a confocal laser microscope (LMS780 spectral confocal system, Zeiss Co., Ltd., Germany).

■ ASSOCIATED CONTENT

Supporting Information

The Supporting Information is available free of charge at https://pubs.acs.org/doi/10.1021/acsomega.2c05042.

Photophysical properties of the compounds, singlet oxygen generation assay of the compounds, evaluation of antitumor activity of I_2BODIPY without GLUT1 ligand, cellular uptake of the compounds in cancer cells, evaluation of bioactivity of talaporfin sodium in cancer cells, and synthetic protocols and spectral data of the compounds (PDF)

■ AUTHOR INFORMATION

Corresponding Author

Hiroyuki Nakamura − *Laboratory for Chemistry and Life Science, Institute of Innovative Research, Tokyo Institute of Technology, Yokohama 226-8503, Japan;* orcid.org/0000-0002-4511-2984; Phone: +81-(0)45-924-5244; Email: hiro@res.titech.ac.jp

Authors

Kazuki Miura − *Laboratory for Chemistry and Life Science, Institute of Innovative Research, Tokyo Institute of Technology, Yokohama 226-8503, Japan;* orcid.org/0000-0003-4514-6305

Yijin Wen − *School of Life Science and Technology, Tokyo Institute of Technology, Yokohama 226-8501, Japan*

Michihiko Tsushima − *School of Life Science and Technology, Tokyo Institute of Technology, Yokohama 226-8501, Japan*

Complete contact information is available at: https://pubs.acs.org/10.1021/acsomega.2c05042

Notes

The authors declare no competing financial interest.

■ ACKNOWLEDGMENTS

This work was supported by AMED, Japan, under grant number 20am0401028h0002, and the fundamental science research support program of the Laboratory for Chemistry and Life Science, Institute of Innovative Research, Tokyo Institute of Technology. We thank Prof. Hideya Yuasa for his useful suggestions on photosensitizers. This work was performed under the research program of the Network Joint Research Center for Materials and Devices: Dynamic Alliance for Open Innovation Bridging Human, Environment and Materials. The authors thank the Biomaterials Analysis Division, Tokyo Institute of Technology, for confocal microscopy analysis and the Open Research Facilities for Life Science and Technology, Tokyo Institute of Technology, for spectrofluorophotometer analysis.

■ REFERENCES

(1) Jay, D. G. Selective destruction of protein function by chromophore-assisted laser inactivation. *Proc. Natl. Acad. Sci. U.S.A.* **1988**, *85*, 5454−5458.

(2) Liao, J. C.; Roider, J.; Jay, D. G. Chromophore-assisted laser inactivation of proteins is mediated by the photogeneration of free radicals. *Proc. Natl. Acad. Sci. U.S.A.* **1994**, *91*, 2659−2663.

(3) Beck, S.; Sakurai, T.; Eustace, B. K.; Beste, G.; Schier, R.; Rudert, F.; Jay, D. G. Fluorophore-assisted light inactivation: a high-throughput tool for direct target validation of proteins. *Proteomics* **2002**, *2*, 247−255.

(4) Rajfur, Z.; Roy, P.; Otey, C.; Romer, L.; Jacobson, K. Dissecting the link between stress fibres and focal adhesions by CALI with EGFP fusion proteins. *Nat. Cell Biol.* **2002**, *4*, 286−293.
(5) Jacobson, K.; Rajfur, Z.; Vitriol, E.; Hahn, K. Chromophore-assisted laser inactivation in cell biology. *Trends Cell Biol.* **2008**, *18*, 443−450.
(6) Takemoto, K. Optical manipulation of molecular function by chromophore-assisted light inactivation. *Proc. Jpn. Acad. Ser. B Phys. Biol. Sci.* **2021**, *97*, 197−209.
(7) Lee, J.; Udugamasooriya, D. G.; Lim, H. S.; Kodadek, T. Potent and selective photo-inactivation of proteins with peptoid-ruthenium conjugates. *Nat. Chem. Biol.* **2010**, *6*, 258−260.
(8) Liu, X.; Dix, M.; Speers, A. E.; Bachovchin, D. A.; Zuhl, A. M.; Cravatt, B. F.; Kodadek, T. J. Rapid development of a potent photo-triggered inhibitor of the serine hydrolase RBBP9. *Chembiochem* **2012**, *13*, 2082−2093.
(9) Sato, S.; Morita, K.; Nakamura, H. Regulation of target protein knockdown and labeling using ligand-directed $Ru(bpy)_3$ photocatalyst. *Bioconjugate Chem.* **2015**, *26*, 250−256.
(10) Sato, S.; Tsushima, M.; Nakamura, H. Target-protein-selective inactivation and labelling using an oxidative catalyst. *Org. Biomol. Chem.* **2018**, *16*, 6168−6179.
(11) Warburg, O. On the origin of cancer cells. *Science* **1956**, *123*, 309−314.
(12) Liberti, M. V.; Locasale, J. W. The warburg effect: How does it benefit cancer cells. *Trends Biochem. Sci.* **2016**, *41*, 211−218.
(13) Chen, X. S.; Li, L. Y.; Guan, Y. D.; Yang, J. M.; Cheng, Y. Anticancer strategies based on the metabolic profile of tumor cells: therapeutic targeting of the Warburg effect. *Acta Pharmacol. Sin.* **2016**, *37*, 1013−1019.
(14) Kozal, K.; Jóźwiak, P.; Krześlak, A. Contemporary perspectives on the warburg effect inhibition in cancer therapy. *Cancer Control* **2021**, *28*, 10732748211041243.
(15) Medina, R. A.; Owen, G. I. Glucose transporters: expression, regulation and cancer. *Biol. Res.* **2002**, *35*, 9−26.
(16) Szablewski, L. Expression of glucose transporters in cancers. *Biochim. Biophys. Acta* **2013**, *1835*, 164−169.
(17) Dolmans, D. E.; Fukumura, D.; Jain, R. K. Photodynamic therapy for cancer. *Nat. Rev. Cancer* **2003**, *3*, 380−387.
(18) Gunaydin, G.; Gedik, M. E.; Ayan, S. Photodynamic therapy for the treatment and diagnosis of cancer-a review of the current clinical status. *Front. Chem.* **2021**, *9*, 686303.
(19) Kato, H.; Furukawa, K.; Sato, M.; Okunaka, T.; Kusunoki, Y.; Kawahara, M.; Fukuoka, M.; Miyazawa, T.; Yana, T.; Matsui, K.; Shiraishi, T.; Horinouchi, H. Phase II clinical study of photodynamic therapy using mono-L-aspartyl chlorin e6 and diode laser for early superficial squamous cell carcinoma of the lung. *Lung Cancer* **2003**, *42*, 103−111.
(20) Muragaki, Y.; Akimoto, J.; Maruyama, T.; Iseki, H.; Ikuta, S.; Nitta, M.; Maebayashi, K.; Saito, T.; Okada, Y.; Kaneko, S.; Matsumura, A.; Kuroiwa, T.; Karasawa, K.; Nakazato, Y.; Kayama, T. Phase II clinical study on intraoperative photodynamic therapy with talaporfin sodium and semiconductor laser in patients with malignant brain tumors. *J. Neurosurg.* **2013**, *119*, 845−852.
(21) Yano, T.; Kasai, H.; Horimatsu, T.; Yoshimura, K.; Teramukai, S.; Morita, S.; Tada, H.; Yamamoto, Y.; Kataoka, H.; Kakushima, N.; Ishihara, R.; Isomoto, H.; Muto, M. A multicenter phase II study of salvage photodynamic therapy using talaporfin sodium (ME2906) and a diode laser (PNL6405EPG) for local failure after chemoradiotherapy or radiotherapy for esophageal cancer. *Oncotarget* **2017**, *8*, 22135−22144.
(22) Mitsunaga, M.; Ogawa, M.; Kosaka, N.; Rosenblum, L. T.; Choyke, P. L.; Kobayashi, H. Cancer cell-selective in vivo near infrared photoimmunotherapy targeting specific membrane molecules. *Nat. Med.* **2011**, *17*, 1685−1691.
(23) Ogawa, M.; Tomita, Y.; Nakamura, Y.; Lee, M. J.; Lee, S.; Tomita, S.; Nagaya, T.; Sato, K.; Yamauchi, T.; Iwai, H.; Kumar, A.; Haystead, T.; Shroff, H.; Choyke, P. L.; Trepel, J. B.; Kobayashi, H. Immunogenic cancer cell death selectively induced by near infrared photoimmunotherapy initiates host tumor immunity. *Oncotarget* **2017**, *8*, 10425−10436.
(24) Kobayashi, H.; Choyke, P. L. Near-infrared photoimmunotherapy of cancer. *Acc. Chem. Res.* **2019**, *52*, 2332−2339.
(25) Shivran, N.; Tyagi, M.; Mula, S.; Gupta, P.; Saha, B.; Patro, B. S.; Chattopadhyay, S. Syntheses and photodynamic activity of some glucose-conjugated BODIPY dyes. *Eur. J. Med. Chem.* **2016**, *122*, 352−365.
(26) Treekoon, J.; Pewklang, T.; Chansaenpak, K.; Gorantla, J. N.; Pengthaisong, S.; Lai, R. Y.; Ketudat-Cairns, J. R.; Kamkaew, A. Glucose conjugated aza-BODIPY for enhanced photodynamic cancer therapy. *Org. Biomol. Chem.* **2021**, *19*, 5867−5875.
(27) Tsushima, M.; Sato, S.; Miura, K.; Niwa, T.; Taguchi, H.; Nakamura, H. Intracellular photocatalytic-proximity labeling for profiling protein-protein interactions in microenvironments. *Chem. Commun.* **2022**, *58*, 1926−1929.
(28) Gould, S. M.; Tawfik, D. S. Directed evolution of the promiscuous esterase activity of carbonic anhydrase II. *Biochemistry* **2005**, *44*, 5444−5452.
(29) Tsuga, Y.; Katou, M.; Kuwabara, S.; Kanamori, T.; Ogura, S. I.; Okazaki, S.; Ohtani, H.; Yuasa, H. A twist-assisted biphenyl photosensitizer passable through glucose channel. *Chem. Asian J.* **2019**, *14*, 2067−2071.
(30) Epelde-Elezcano, N.; Prieto-Montero, R.; Martínez-Martínez, V.; Ortiz, M. J.; Prieto-Castañeda, A.; Peña-Cabrera, E.; Belmonte-Vázquez, J. L.; López-Arbeloa, I.; Brown, R.; Lacombe, S. Adapting BODIPYs to singlet oxygen production on silica nanoparticles. *Phys. Chem. Chem. Phys.* **2017**, *19*, 13746−13755.
(31) Li, Z. Y.; Shi, Y. L.; Liang, G. X.; Yang, J.; Zhuang, S. K.; Lin, J. B.; Ghodbane, A.; Tam, M. S.; Liang, Z. J.; Zha, Z. G.; Zhang, H. T. Visualization of GLUT1 trafficking in live cancer cells by the use of a dual-fluorescence reporter. *ACS Omega* **2020**, *5*, 15911−15921.
(32) Naftalin, R. J.; Afzal, I.; Cunningham, P.; Halai, M.; Ross, C.; Salleh, N.; Milligan, S. R. Interactions of androgens, green tea catechins and the antiandrogen flutamide with the external glucose-binding site of the human erythrocyte glucose transporter GLUT1. *Br. J. Pharmacol.* **2003**, *140*, 487−499.
(33) Ung, P. M.; Song, W.; Cheng, L.; Zhao, X.; Hu, H.; Chen, L.; Schlessinger, A. Inhibitor discovery for the human GLUT1 from homology modeling and virtual screening. *ACS Chem. Biol.* **2016**, *11*, 1908−1916.
(34) Oh, S.; Kim, H.; Nam, K.; Shin, I. Glut1 promotes cell proliferation, migration and invasion by regulating epidermal growth factor receptor and integrin signaling in triple-negative breast cancer cells. *BMB Rep.* **2017**, *50*, 132−137.
(35) Aizawa, K.; Okunaka, T.; Ohtani, T.; Kawabe, H.; Yasunaka, Y.; O'Hata, S.; Ohtomo, N.; Nishimiya, K.; Konaka, C.; Kato, H.; Hayata, Y.; Saito, T. Localization of mono-L-aspartyl chlorin e6 (NPe6) in mouse tissues. *Photochem. Photobiol.* **1987**, *46*, 789−793.
(36) Algorri, J. F.; Ochoa, M.; Roldán-Varona, P.; Rodríguez-Cobo, L.; López-Higuera, J. M. Photodynamic therapy: A compendium of latest reviews. *Cancers* **2021**, *13*, 4447.
(37) Sato, S.; Nakamura, H. Ligand-directed selective protein modification based on local single-electron-transfer catalysis. *Angew. Chem., Int. Ed.* **2013**, *52*, 8681−8684.

https://doi.org/10.1021/acsomega.2c05042
ACS Omega 2022, 7, 34685−34692